International Journal of Biological Macromolecules 133 (2019) 867–874

Contents lists available at ScienceDirect

International Journal of Biological Macromolecules

journal homepage: http://www.elsevier.com/locate/ijbiomac

Chitosan enhances calcium carbonate precipitation and solidification mediated by bacteria

Thiloththama Hiranya Kumari Nawarathna [a], Kazunori Nakashima [b,*], Satoru Kawasaki [b]

[a] Division of Sustainable Resources Engineering, Graduate School of Engineering, Hokkaido University, Kita 13, Nishi 8, Kita-Ku, Sapporo 060-8628, Japan
[b] Division of Sustainable Resources Engineering, Faculty of Engineering, Hokkaido University, Kita 13, Nishi 8, Kita-Ku, Sapporo 060-8628, Japan

ARTICLE INFO

Article history:
Received 30 November 2018
Received in revised form 1 April 2019
Accepted 24 April 2019
Available online 25 April 2019

Keywords:
Biomineral
Calcium carbonate
Chitosan
Hydrogel
Morphology

ABSTRACT

Formation of the biominerals in living organisms is mainly associated with organic macromolecules. These organic materials play an important role in the nucleation, growth, and morphology controls of the biominerals. Current study mimics this concept of organic matrix- mediated biomineralization by using microbial induced carbonate precipitation (MICP) method in combination with the cationic polysaccharide chitosan. $CaCO_3$ precipitation was performed by the hydrolysis of urea by the ureolytic bacteria *Pararhodobacter* sp. SO1 in the presence of $CaCl_2$, with and without chitosan. The crystal polymorphism and morphology of oven-dried samples were analyzed by X-ray diffraction and scanning electron microscopy. The amount of precipitate obtained was higher in the presence of chitosan. The precipitate included both of the $CaCO_3$ and the chitosan hydrogel. Rhombohedral crystals were dominant in the precipitate without chitosan and distorted crystal agglomerations were found with chitosan. Sand solidification experiments were conducted in the presence of chitosan under different experimental conditions. By adding chitosan, more strongly cemented sand specimens could be obtained than those from conventional method. All of these results confirm the positive effect of chitosan for the $CaCO_3$ precipitation and sand solidification.

1. Introduction

Biomineralization is the formation of minerals in biological systems. It is a combined approach to study of the biologically-formed materials and processes that lead to the construction of hierarchically structured composite materials [1]. Biominerals provide protection, structural support, and mechanical strength for the organisms. Calcium is the most common biomineral available in nature and is the main constituent of skeletal structures. The formation of biominerals is mainly associated with the organic macromolecules, which control the habit, polymorphism, and morphology of the crystals [2,3]. In comparison with the natural minerals, organic-inorganic hybrid materials have distinctive optical properties and higher mechanical strength [3,4].

Nacre of the Mollusca is one of the best examples available in nature for biogenic mineral formation. In nacre, aragonitic $CaCO_3$ is deposited upon the organic matrix of silk- fibroin like protein and polysaccharide chitin [5,6], providing an inorganic-organic hierarchical structure with higher strength [2]. Chitin is a one of the most abundant natural biopolymer, which can be found in the exoskeleton of arthropods, marine diatoms, and certain types of algae [7–10]. However, chitin has limited number of field applications due to its huge insolubility and complications in processing. Hence, a number of byproducts are developed from chitin, which can be used readily for field applications.

Chitosan is the most important derivative of chitin, which is obtained by the deacetylation of chitin. It is a linear poly cationic biopolymer and is positively charged in the acidic environment [9,11,12]. Its biodegradability, biocompatibility, and low toxicity make it appropriate for a number of applications in medicine, agriculture, cosmetic, and waste water engineering field [12–15]. However, very limited number of research studies have been carried out earlier regarding the applicability of chitosan in civil engineering.

Our interest is in the use of chitosan as an organic additive, to mimic the organic matrix-mediated biomineralization, combining with microbial induced carbonate precipitation method (MICP). MICP is a biocatalytic $CaCO_3$ production/precipitation system by the hydrolysis of urea using urease as shown in the following Eqs. (1)–(3) [16–20]. Urease is a multi-subunit, nickel containing enzyme that can be found in some bacterial species and plants [21].

$$CO(NH_2)_2 + H_2O \xrightarrow{\text{Urease}} H_2NCOO^- + NH_4^+ \quad (1)$$

$$H_2NCOO^- + H_2O \rightarrow HCO_3^- + NH_3 \quad (2)$$

* Corresponding author.
E-mail addresses: nakashima@geo-er.eng.hokudai.ac.jp (K. Nakashima), kawasaki@geo-er.eng.hokudai.ac.jp (S. Kawasaki).

https://doi.org/10.1016/j.ijbiomac.2019.04.172
0141-8130/

$$Ca^{2+} + HCO_3^- + NH_3 \rightarrow CaCO_3 + NH_4^+ \quad (3)$$

Recently, MICP has attracted much attention as a challenging and ecofriendly ground improvement method. Previous research has revealed that MICP can increase the soil strength and stiffness with minimum disturbance to the soil [22–24]. Introducing organic materials into the MICP process would be more effective to improve the efficiency of the process. We have to consider the number of factors before implement. Basically, the organic materials should not inhibit the bacterial as well as enzyme activity. Also, effect of the organic matters on the $CaCO_3$ crystallization should be studied. Due to these difficulties very little amount of research works have been carried out earlier under this area. One research group has studied the polymer-modified MICP for sand solidification by using polyvinyl alcohol (PVA). They obtained higher strength and higher amount of $CaCO_3$ by using polymer-modified MICP than the conventional MICP. Moreover, they found that cementation solution containing PVA produced framboidal shape vaterite crystals while water-based MICP method provided rhombohedral shape calcite crystals [25]. In our previous research, we found that the cationic polypeptide poly-lysine has the ability to increase $CaCO_3$ precipitation rate as well as strength of cemented sand specimen compared to that of conventional MICP [26].

Instead of MICP, some of previous research works can be found based on polymer-modified enzyme induced carbonate precipitation (EICP). In EICP, extracted urease enzyme was used instead of microbial whole-cell urease. Previous research works found that xanthan gum and guar gum-modified EICP does not obstruct the $CaCO_3$ precipitation and obtained higher unconfined compressive strength (UCS) value than that of without biopolymers [27]. Poly (acrylic acid) (PAA) have successfully worked with EICP and performed well for soil stabilization. By combing PAA with EICP stiffness and strength of the soil can be improved significantly [28].

This work is addressing the use of chitosan to improve the efficiency of MICP process. Chitosan is an inexpensive natural biopolymer. Hence, the use of chitosan would help to produce more ecofriendly and green materials. On the other hand, the effects of soluble organic macromolecules on $CaCO_3$ crystallization have also been studied widely [29,30] however, there are few reports on the use of insoluble organic materials to control $CaCO_3$ crystallization, mainly focusing on the formation of $CaCO_3$ thin film [9,14,31]. This study is the first investigation addressing the effects of a cationic polysaccharide, chitosan, on $CaCO_3$ crystallization using MICP.

2. Materials and methods

2.1. Materials

2.1.1. Chemical reagents and organic materials

Polypeptone was purchased from Nihon Seiyaku Co. Ltd. (Tokyo, Japan) and $FePO_4$ was bought from Junsei Chemical Co. Ltd. (Tokyo, Japan). Yeast extract and nutrient broth were obtained from BD Biosciences Advanced Bioprocessing company, USA. Chitosan (degree of deacetylation – 80%) was purchased from the Wako Pure Chemical Industries Ltd. (Tokyo, Japan). All other organic materials and chemical reagents were purchased from the Wako Pure Chemical Industries Ltd. (Tokyo, Japan).

2.1.2. Sand

Commercially available Mikawa sand was used for our experiments. Mean diameter of sand is 0.87 mm and particle density is 2.66 g/cm^3. Coefficient of uniformity (C_u) and coefficient of curvature (C_c) of Mikawa sand are 1.27 and 0.97. Sand can be classified as poorly graded sand according to the unified soil classification system (USCS).

2.2. Preparation of bacterial cell culture

The ureolytic bacterium, *Pararhodobacter* sp. SO1, which is a gram-negative bacterium with high urease activity [17,32], isolated from beach sand in Sumuide, Nago, Okinawa [33], was used in this study. The bacterial cells were pre-cultured in Zobell 2216E medium (polypeptone 5.0 g/L, yeast extract 1.0 g/L, $FePO_4$ 0.1 g/L in artificial seawater, pH 7.6–7.8; 5 mL) by shaking at 30 °C and 160 rpm for 24 h. The pre-culture (1 mL) was inoculated into fresh Zobell 2216E medium (100 mL). The mixture was kept in the shaking incubator under the same conditions as those used for the pre-culturing, for 48 h. The cells were collected by centrifugation (10 °C, 6300 ×*g*, 5 min) of the bacterial culture. The cells were resuspended in sterilized water to adjust the cell concentration ($OD_{600} = 1$). The cell concentration was determined by UV–visible spectroscopy (V-730, JASCO Corporation, Tokyo, Japan) as an optical density value measured at 600 nm wave length (OD_{600}).

2.3. Precipitation of $CaCO_3$ crystals

A solution of 1% chitosan was obtained by dissolving the chitosan powder in 1% acetic acid solution. After complete dissolution, the chitosan solution was neutralized at pH 6.8 by using 0.1 M NaOH solution. *Pararhodobacter* sp. SO1 cells were added to a substrate solution containing urea (0.3 mol/L) and $CaCl_2$ (0.3 mol/L), in the presence or absence of chitosan. The reaction mixture (10 mL) was shaken at 30 °C and 160 rpm for 24 h. The samples were centrifuged (24 °C, 14200 ×*g*, 10 min) to separate the $CaCO_3$ precipitate from the supernatant. The precipitates were dried in an oven at 90 °C for 24 h, and then the dry weights of the precipitates were determined. Experiments were conducted at various bacterial concentrations ($OD_{600} = 0.01$–0.1) in the presence (0.03%) or absence of chitosan. The same reaction was conducted at various chitosan concentrations (0–0.15%) with the bacterial concentration of $OD_{600} = 0.1$. All experiments were done in triplicate and mean value was plotted. Standard deviation was used to represent the error bars.

2.4. Sand solidification in syringe

Sand solidification experiments were conducted using the method previously described [32] with or without chitosan, to evaluate the effect of chitosan on sand solidification. Laboratory scale model experiments were conducted using 35 mL syringe (mean diameter $D_{50} =$ 2.5 cm and height 7 cm). Oven dried (110 °C, 48 h) Mikawa sand was placed in to the syringe as three layers and each layer was subjected to 20 hammer blows. Firstly, the bacteria suspension (16 mL, $OD_{600} = 1$) was injected into the syringe and kept 5–10 min to allow fixation of the bacteria to sand particles. Subsequently, the cementation solution (20 mL; 0.3 M urea, 0.3 M $CaCl_2$, 0.02 M sodium hydrogen carbonate, 0.2 M ammonium chloride, and 3 g/L nutrient broth) was injected into the syringe and the solution drained out from the outlet, leaving 2 mL of the solution above the surface to maintain the sand in immersed condition.

The experiments were conducted under various concentrations of chitosan and various bacteria injection intervals as given in Table 1. In one set, the bacteria were injected only once on the first day and the chitosan was injected on the 8th day. In another set, the bacteria were injected twice, i.e., on the first day and again after 7 days, and the chitosan was injected on the 11th day. After 14 days curing time, UCS of the samples were determined with a needle penetration device (SH70, Maruto Testing Machine Company, Tokyo, Japan). Calibration Eq. (4) given by the manufacture was used to estimate the UCS value which has been developed by considering 114 natural rock samples and 50 improved soils with cements. All experiments were done in triplicate and mean value was plotted. Standard deviation was used to represent the

Table 1
Experimental conditions for sand solidification.

	Chitosan	Bacterial injection
S1	–	Once[b]
S2	0.15%[a]	Once[b]
S3	0.3%[a]	Once[b]
S4	–	Twice[c]
S5	0.15%[a]	Twice[c]
S6	0.3%[a]	Twice[c]

[a] Initial concentration of the chitosan solution applied to the column in the solidification test.
[b] Injection of bacterial culture only at the beginning of the solidification test.
[c] Injection of bacterial culture at the beginning and after 7 days of the solidification test.

error bars.

$$\log(y) = 0.978\ \log(x) + 2.621 \quad (4)$$

x = Penetration gradient (N/mm)
y = Unconfined compressive strength

2.5. X-ray diffraction and scanning electron microscopy analyses

Morphology of the precipitated $CaCO_3$ crystals was investigated by using scanning electron microscopy (SEM; Miniscope TM3000, Hitachi, Tokyo, Japan). X-ray diffraction (XRD; MiniFlex™, Rigaku Co., Ltd., Tokyo, Japan) analysis was conducted to identify the polymorphs of the precipitated $CaCO_3$.

3. Results and discussion

3.1. Effect of chitosan on $CaCO_3$ precipitation

The amount of precipitate formed by ureolytic bacterial at different bacteria concentrations in the presence or absence of chitosan is given in Fig. 1. In both the conditions, the amount of precipitate increased with the bacterial concentration. In MICP process, the $CaCO_3$ formation efficiency mainly depends on the urease activity of the relevant bacteria and a higher urease activity is favorable for the formation of higher amounts of $CaCO_3$ [34]. The increase in urease activity of the *Pararhodobacter* sp. SO1 with increasing cell concentration caused rapid nucleation and growth of $CaCO_3$ crystals, and produced larger amounts of $CaCO_3$ [19,26]. And also, maximum urease activity of the *Pararhodobacter* sp. SO1 was found around pH 8 [19] and this pH value is favorable for the $CaCO_3$ crystallization [35,36].

Higher amount of precipitate could be obtained in the system with chitosan than in that without chitosan. The effect of chitosan was clearer at lower bacterial concentrations and significant effect was not

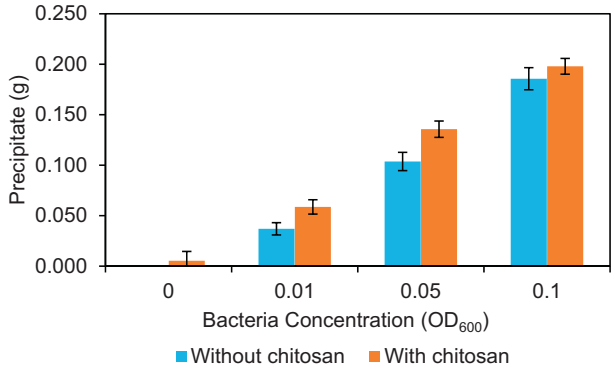

Fig. 1. Amounts of precipitate formed at various bacterial concentrations (OD_{600}) with or without the addition of chitosan. Error bars show the standard deviation of the values from three independent experiments.

discovered at higher cell concentrations. The results are consistent with our previous study using cationic polypeptide (poly-Lysine). At higher cell concentrations, bacterial activity would be a dominant factor than the effect of the bio-polymer [26]. The precipitate with chitosan was mainly composed of two components, precipitated $CaCO_3$ and the precipitated chitosan hydrogel. Chitosan is a cationic polysaccharide with pKa of approximately 6.5 [11,37,38]. Hence, the amino groups of the chitosan are positively charged in the acidic environment [9,11]. When increasing the pH above 6.5, chitosan tends to form its hydrogel due to the deprotonation of the amino groups [12,38]. In the present reaction mixture, ammonia was formed due to the hydrolysis of urea, which leads to pH increase to approximately 7.1. This weak alkaline condition is favorable for the chitosan to form its hydrogel by the hydrogen bonds and hydrophobic interaction between molecules [12,13].

Most of the acidic polypeptides inhibit $CaCO_3$ nucleation and growth [30,39], while basic polypeptides promote the growth and nucleation of crystals [26,30]. Chitosan also promotes the $CaCO_3$ nucleation and growth. Interaction between the chitosan and calcite is difficult to explain. However, it may not be only by electrostatic interactions because chitosan is mostly electroneutral under weak alkaline condition.

Fig. 2 shows the morphologies of the crystals in the presence of chitosan at various bacterial concentrations. In our previous work, we examined the effect of the bacterial cell concentration on the morphology of the crystals without any organic additives [26]. Rhombohedral calcite crystals were dominant in precipitate without the organic additives and the size of the crystals reduced with the increase in the cell concentration. In $CaCO_3$ crystallization, bacterial cells themselves act as a nucleation site for the $CaCO_3$ crystals. Hence, a smaller number of crystals were formed at lower bacteria concentration due to the lack of sufficient nucleation sites. In contrast, a larger number of small crystals were produced at higher bacterial concentrations since each cell acts as a nucleation site. Even though chitosan speeds up the $CaCO_3$ nucleation and growth process, $CaCO_3$ can nucleate and growth efficiently without chitosan also.

At lower bacteria concentrations ($OD_{600} = 0.01$), good rhombohedral crystals were precipitated with the chitosan hydrogel as shown in the Fig. 2(a). However, the crystal shape deformed gradually with the increase in the cell concentration. Finally, at higher bacterial cell concentrations ($OD_{600} = 0.1$), distorted-shaped larger crystals with poly crystalline particles were formed as shown in Fig. 2(c). Moreover, spherical crystals can be seen at higher cell concentrations.

Chitosan has a good ability to make complexes with certain metal ions. The amino groups as well as the hydroxyl groups present in chitosan are known to contribute to the metal adsorption through chelation and sorption [40,41]. Ca^{2+} can absorb into the chitosan hydrogel by hard acid-hard base reaction. According to the Lewis acid-base classification, Ca^{2+} is classified as a hard acid and R-NH_2 groups classified as hard base [42]. Due to this acid-base interaction, Ca^{2+} ions are embedded in to the chitosan hydrogel and provide nucleation sites for the $CaCO_3$ crystals to nucleate and grow [43].

At lower bacterial cell concentrations, lower amount of CO_3^{-2} was produced due to the lower urease activity. Hence, well-developed rhombohedral crystals with individual chitosan hydrogel were obtained at lower cell concentration as shown in Fig. 2(a). The higher bacterial cell concentrations produced higher amount of $CaCO_3$ precipitate due to higher urease activity. This led to the formation of distorted-shaped larger crystals due to the agglomeration of individual crystals. However, the polycrystalline particles which appeared on the crystal surface may be due to the binding of the -OH and -NH_2 functional groups of the chitosan on to the surface of the crystals; they inhibited the growth of free crystals and aggregated to form the polycrystalline particles [43]. According to the XRD pattern given in Fig. 3, the spherical particles present in Fig. 2(c-1) can be classified as a vaterite. Similar shape of vaterite was found by other studies, where $CaCO_3$ was formed by chemical precipitation [44,45].

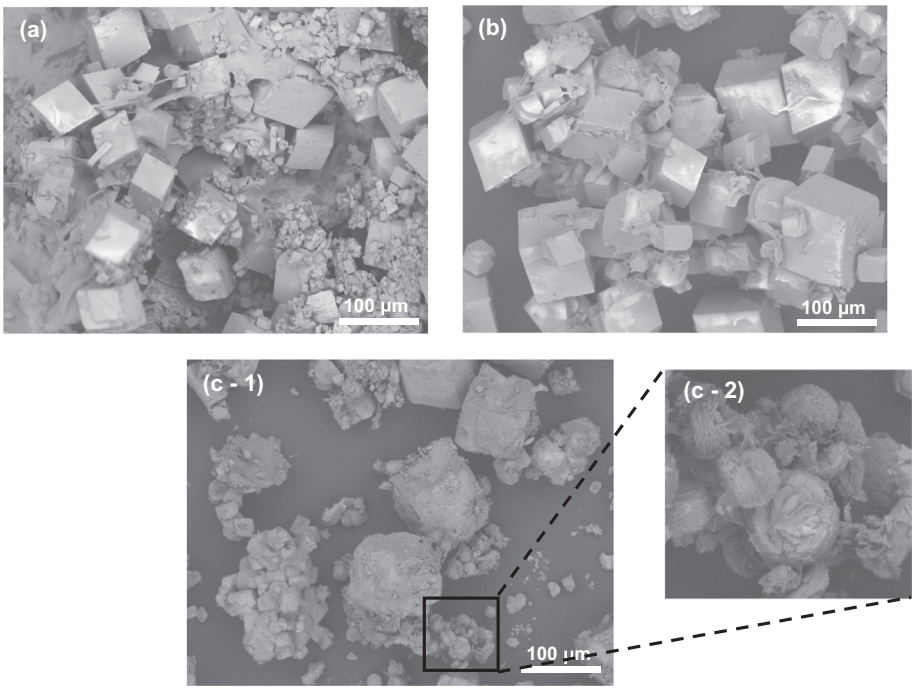

Fig. 2. SEM images of $CaCO_3$ precipitates at various bacterial concentrations with chitosan (0.03%): (a) $OD_{600} = 0.01$, (b) $OD_{600} = 0.05$, (c-1) $OD_{600} = 0.1$, (c-2) spherical vaterite crystals.

Most of the $CaCO_3$ crystals generated by the MICP are calcite with the morphology of elongated, rhombohedral, polyhedron, trigonal prism or rod-shaped crystals [26,46–48]. Generation of spherical crystals is an exceptional case and mostly these spherical crystals are vaterite. However, spherical vaterite crystals have been obtained by some of previous studies by introducing the organic materials into the MICP process. Incorporating sodium alginate into the MICP process formed vaterite crystals and hexagonal, spherical and capsule-shaped vaterite crystals have been obtained by varying the sodium alginate concentration [49]. In addition, spherical vaterite crystals have been obtained by PVA modified MICP [25]. Vaterite is metastable phase of the $CaCO_3$ polymorphism and easily transformed to the stable form such as calcite or aragonite. Supersaturation is the main governing factor for the formation of vaterite crystals. At higher supersaturation most soluble and least stable form of polymorphism form first [50,51]. Generally, when the viscosity of the reaction mixture is higher, it promotes the enrichment of local ion concentration and hence increase the supersaturation [52]. Thus, the viscosity of the reaction mixture increased in the presence of chitosan, leading to the supersaturation and the formation of vaterite crystals.

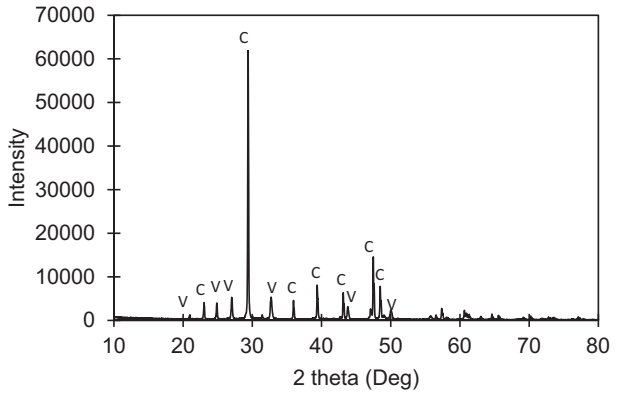

Fig. 3. XRD patterns of $CaCO_3$ precipitates with chitosan (bacteria concentration $OD_{600} = 0.1$, chitosan concentration = 0.03%) C: calcite; V: vaterite.

On the other hand, organic materials promote the formation and stabilizing of vaterite crystals [30,53,54]. Organic materials interact with the calcium and carbonate ions in the solution and reduce the concentration of free ions in the bulk solution. Therefore, it reduces the nucleation rate and promote the formation of vaterite crystals [51]. Similarly, in the presence of chitosan, Ca^{2+} ions attached to the chitosan hydrogel and reduced the available free ions in the solution which promote the formation of metastable form of polymorphism. In addition, previous research works found that strong interaction between the amide groups of the organic material and veratite surface promote the long-term stabilization of vaterite [55].

Selection of the appropriate calcium source is also very important in MICP related research works. Mainly calcium source should not inhibit the bacterial growth as well as it should not interfere with the enzyme activities. Compared with the other calcium sources such as calcium acetate, calcium nitrate, calcium oxalate, calcium chloride is the most effective reagent for calcium carbonate precipitation using microbial activities. Previous studies found that $CaCl_2$ increased the urease activity of the *Bacillus* sp. CR2 more efficiently than other calcium sources. Furthermore, $CaCl_2$ gave higher amount of calcite precipitation [56]. In addition, more consolidated sand column can be obtained by adding $CaCl_2$ compared with the other calcium sources [57]. By considering these results, $CaCl_2$ was used as the calcium source for our experiments.

3.2. Effect of chitosan concentration

Fig. 4 shows the amounts of precipitate formed at different concentrations of chitosan. The amount of precipitate increased slightly with the chitosan concentration. When increasing the chitosan concentration, the increase in the amount of precipitate mainly occurred due to the increase in chitosan hydrogel rather than the $CaCO_3$ precipitate. At higher chitosan concentrations, more chitosan chains are present in the solution, and the distance between the chains decreases, leading to easy interaction between the chains and formed higher amounts of precipitates through inter molecular hydrogen bonds [58]. The morphology of the precipitated crystals are shown in Fig. 5. Both the polyhedron and spherical crystals were obtained at lower chitosan concentrations. The distorted-shaped spherical and polyhedron crystals

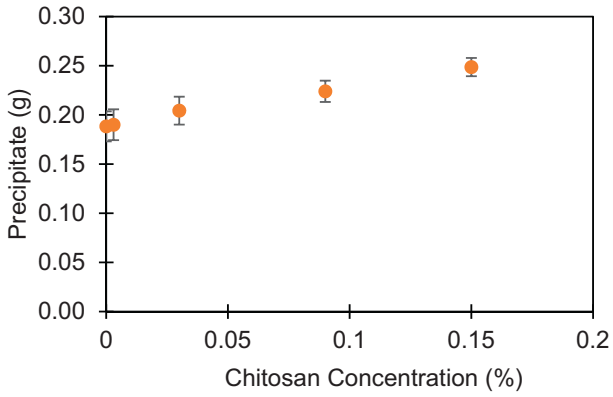

Fig. 4. Variations in the amount of calcium carbonate precipitated with the changes in chitosan concentration. Error bars show the standard deviation of the values from three independent experiments.

can be seen at the intermediate chitosan concentrations. At higher chitosan concentrations, the larger size polyhedron-type crystals and individual chitosan hydrogel were obtained. The formation of the larger size distorted-shape crystals with the increase in the chitosan concentration may be due to the adsorption of the functional groups of the chitosan onto the crystals surface [43].

According to the XRD results shown in the Fig. 3, the precipitate with chitosan produced both the calcite and vaterite crystals. These XRD results are similar to that for the condition in Fig. 5(b) (OD_{600} = 0.1 and chitosan concentration 0.03%). Hence, the spherical crystals in Fig. 5 (a) and Fig. 5(b) most probably could be vaterite. Vaterite is the least stable form of $CaCO_3$ with the highest solubility, so it precipitates first and then transforms in to stable calcite, following the solution mediated-transformation [59]. Hence, the morphology change with the increase in the chitosan concentration can be due to the conversion of the metastable phase of the crystals into a more stable form. Initially, both the vaterite and calcite phases precipitated simultaneously due to high solid content and limited diffusivity [60]. Then, the metastable phase started to dissolve and re-precipitated upon the stable calcite crystals as shown in Fig. 5(b). The dissolution of the vaterite starts when the supersaturation drops below the value of its solubility [60]. It appears that higher chitosan concentrations accelerate the conversion of the metastable phase into a stable phase.

Similarly, different polymorphisms and morphologies have been obtained by chemical precipitation of $CaCl_2$ and sodium carbonate (Na_2CO_3) under different experimental conditions. Parakhonskiy et al. [61] successfully obtained the isotropic (spherical and cubic) and anisotropic (elliptical and star-like) crystals by varying the salt concentration and slow down the process by adding ethylene glycol. And also, vaterite crystals have been obtained by introducing poly-L-glutamic acid (pGlu) and poly-L-aspartic acid (pAsp) in to the reaction mixture while mostly cubic calcite crystals were obtained without organic materials. [29,62]

3.3. Sand solidification in syringe

Six sets of experiment (S1–S6) were performed with/without chitosan addition and with various bacterial injection intervals and various chitosan concentrations. The injection of the chitosan simultaneously with the bacteria gave negative results in the solidification and it appears that chitosan is toxic for the bacteria. Hence, we used different time schedules for the injection of bacteria and chitosan.

The estimated UCS values for the solidified samples are shown in Fig. 6. According to the measured UCS values, all of the sand specimens have strength in the range of 1–3 MPa. Hence, all specimens can be classified as strongly cemented according to the classification system proposed by Shafii and Clough [63]. In this classification system, the cemented soils with UCS value between 1 and 3 MPa are classified as

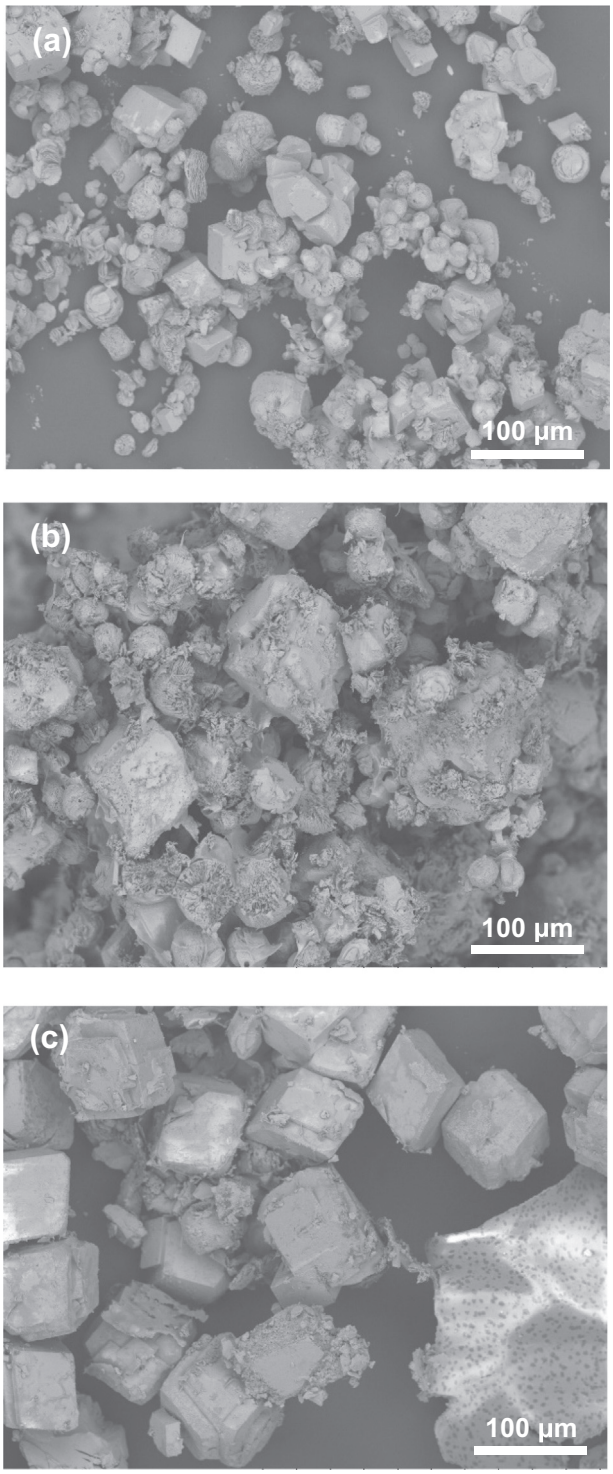

Fig. 5. SEM images of $CaCO_3$ precipitated by bacteria (OD_{600} = 0.1) at different chitosan concentrations: (a) 0.003%, (b) 0.03% and (c) 0.15%.

strongly cemented soil and a UCS value >3 are classified as soft rocks. For all the specimens, a higher strength could be achieved by the reinjection of bacteria after 7 days compared to the single injection. In the case of reinjection of bacteria 96% of strength increment was achieved for the top of the sample by adding chitosan. Without chitosan strength increment was around 76%. In previous studies found that amount of $CaCO_3$ precipitated is directly related to the measured UCS value [23,24,64]. Reinjection of bacteria helped to maintain higher urea hydrolysis rate throughout the experimental period, which led to higher

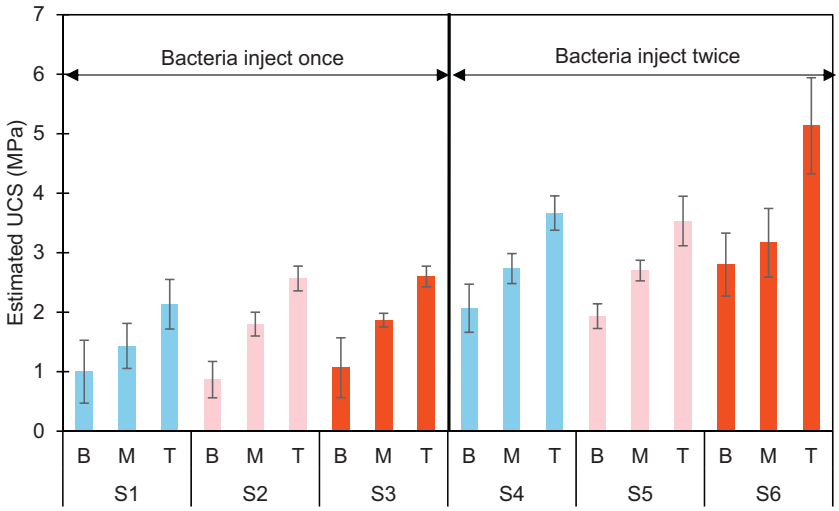

Fig. 6. Estimated UCS values of solidified sand specimens. Error bars show the standard deviation of the values from three independent experiments. S1 and S4: without addition of chitosan, S2 and S5: with addition of chitosan at a concentration of 0.15%, S3 and S6: with addition of chitosan at a concentration of 0.3%.

$CaCO_3$ precipitation and better cementation between the sand particles [26].

Another remarkable point is the decrease in the strength of the solidified sand specimen, from the top to the bottom. It is mainly because of the accumulation of the bacteria at the top of the sample, which leads to higher urease activity near the inlets. This causes the higher precipitation and higher cementation near the top of the specimen and a gradual decrease in the strength along the length of the sample. The lack of oxygen at the bottom of the sand column could possibly inhibit the bacteria activity, because *Pararhodobacter* sp. SO1 are aerobic bacteria and oxygen concentration of the surrounding environment plays a vital role in the bacterial activity [17].

The most important finding of this research is the positive effect of the chitosan on sand solidification. By introducing chitosan, well cemented sand specimens could be obtained and the effect is clearer at higher chitosan concentrations. By introducing chitosan, UCS of the top of the sample increased by 38% compared with the case without chitosan. To achieve better cementation during the sand solidification, the pore spaces between the sand particles should be filled sufficiently by effective bridge between the sand particles [65]. This point-to-point inter-particle contact is very important to achieve higher strength [16]. As mentioned before, chitosan formed its hydrogel under the alkaline conditions. This hydrogel helped to form better bridge between the sand particles. The higher chitosan concentrations led to form thicker hydrogels, which improved the formation of bridge; hence, a better cementation and higher strength could be achieved. Another point to note is, when using chitosan for sand solidification it is better to select a best time to introduce chitosan into the sand column. Introduction of chitosan at the beginning of the experiment did not give good results due to the early formation of chitosan hydrogel. This blocked the penetration of the cementation solution. Hence, better cementation could not be achieved due to the lack of precipitated $CaCO_3$. Similar to in the bridge formation, the amount of precipitated $CaCO_3$ was also important to achieve better mechanical strength [23,66]. In the experiment with bacterial injection twice, the injection of the chitosan on the 11th day was successful and the injection of the chitosan during the 8th day was productive for the specimens with single dose of bacterial injection.

According to the SEM images shown in Fig. 7(a), without the addition of chitosan, the cementation mainly occurred at the contact point. This is mainly due to the lower adsorption of bacteria onto the sand surface. In the specimen of with chitosan, the entire sand surface was covered with $CaCO_3$ crystals as shown in the Fig. 7(b). Chitosan itself acts as a template for $CaCO_3$ crystals to nucleate which led to the distribution of the $CaCO_3$ throughout the sand surface and provided a better cementation than the conventional one. In addition, the formation of the chitosan hydrogel provides extra support to make better bridge between the sand particles as shown in the Fig. 7(b-2). It helps efficient precipitation of $CaCO_3$ by preventing heterogeneous precipitation. Hence higher strength could be achieved by adding chitosan than the conventional MICP.

4. Conclusions

The effects of the cationic polysaccharide chitosan on $CaCO_3$ crystallization and sand solidification was analyzed by using the MICP method. It was found that chitosan has a positive effect on $CaCO_3$ crystallization and sand solidification. Higher amounts of the precipitate could be obtained upon chitosan addition than without adding chitosan. Chitosan also precipitated as its hydrogel with the $CaCO_3$ crystals. XRD results confirmed that precipitate with chitosan has both the calcite and vaterite crystals, while the specimen without chitosan produced only calcite crystals. Increase of the supersaturation in a reaction mixture by adding chitosan leads to the formation of vaterite instead of calcite, which is the most common type of polymorphism in MICP. At lower bacterial concentrations, the precipitate consisted of good rhombohedral crystals and individual chitosan hydrogel. However, higher chitosan concentrations, distorted the crystal shape, and crystal agglomerates were produced. Chitosan act as a template for the $CaCO_3$ crystals to nucleate due to adsorption of the Ca^{2+} ions onto the chitosan hydrogel. In contrast, in the case of without chitosan bacteria cells themselves act as nucleation site for $CaCO_3$ crystals to nucleate and growth. Even though without chitosan also $CaCO_3$ can nucleate and grow efficiently but process could be accelerated effectively by adding chitosan. The higher chitosan concentrations accelerate the conversion of metastable phase of vaterite into the stable phase of calcite. In addition, the chitosan hydrogel assisted in the formation of better bridge between the sand particles. Hence, by adding chitosan better cementation and strength could be achieved than the conventional method. Finally, chitosan can be used to produce good organic-inorganic hybrid green materials, which can be used in a number of civil engineering applications.

Conflicts of interest

There are no conflicts to declare.

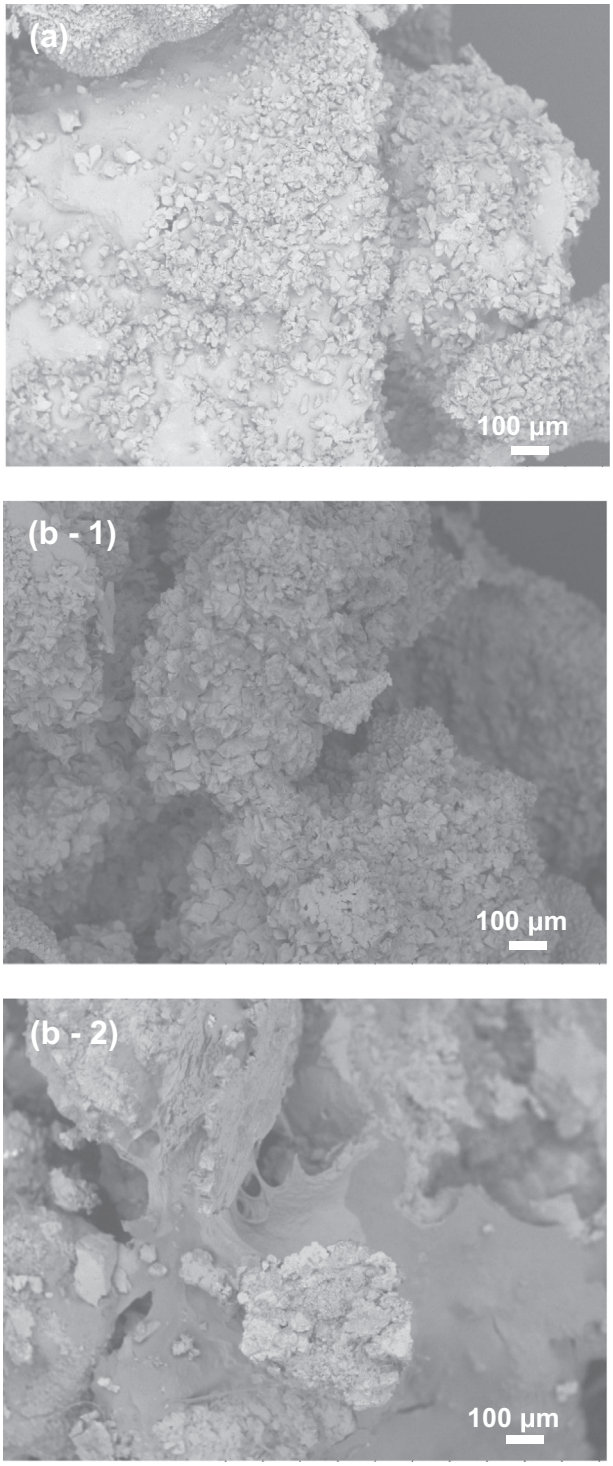

Fig. 7. SEM images of the cemented sand samples: without chitosan (a) and with chitosan (0.3%; b-1, b-2).

Acknowledgements

This work was partly supported by JSPS KAKENHI Grant Number JP15K18273 and JP16H04404.

Author contributions

The experiments were designed by Thiloththama Hiranya Kumari Nawarathna, Kazunori Nakashima and Satoru Kawasaki. T. H. K. Nawarathna carried out the experiments and wrote the manuscript. K. Nakashima and S. Kawasaki supervised the whole project.

References

[1] L.A. Estroff, Biomineralization, Chem. Rev. 108 (11) (2008) 4329−4331, https://doi.org/10.1021/cr8004789.
[2] S. Mann, Biomineralization: Principles and Concepts in Bioinorganic Materials Chemistry, Oxford University Press, Oxford, U.K., 2001
[3] T. kato, T. Suzuki, T. Amamiya, T. Lrie, Effects of macromolecules on the crystallization of $CaCO_3$ the formation of organic/inorganic composite, Supramol. Sci. 5 (3–4) (1998) 411−415, https://doi.org/10.1016/S0968-5677(98)00041-8.
[4] N. Hosoda, T. Kato, Thin-film formation of calcium carbonate crystals: effects of functional groups of matrix polymers, Chem. Mater. 13 (2) (2001) 688−693, https://doi.org/10.1021/cm000817r.
[5] N.H. Munro, K.M. McGrath, Biomimetic approach to forming chitin/aragonite composites, Chem. Commun. 48 (2012) 4716−4718, https://doi.org/10.1039/C2CC00135G.
[6] N.H. Munro, D.W. Green, A. Dangerfield, K.M. McGrath, Biomimetic mineralization of polymeric scaffolds using a combined soaking and kitano approach, Dalton Trans. 40 (2011) 9259–9268, https://doi.org/10.1039/C1DT11056J.
[7] D. Raafat, H.G. Sahl, Chitosan and its antimicrobial potential-a critical literature survey, Microb. Biotechnol. 2 (2) (2009) 186−201, https://doi.org/10.1111/j.1751-7915.2008.00080.x.
[8] R. Nistico, Aquatic-derived biomaterials for a sustainable future: a European opportunity, Resources 6 (4) (2017) 65, https://doi.org/10.3390/resources6040065.
[9] T. Jozwiak, U. Filipkowska, P. Szymczyk, A. Mielcarek, Sorption of nutrients (orthophosphate, nitrate III and V) in an equimolar mixture of P–PO_4, N–NO_2 and N–NO_3 using chitosan, Arab. J. Chem. (2016)https://doi.org/10.1016/j.arabjc.2016.04.008 article in press.
[10] T.L. Yang, Chitin-based materials in tissue engineering: applications in soft tissue and epithelial organ, Int. J. Mol. Sci. 12 (3) (2011) 1936−1963, https://doi.org/10.3390/ijms12031936.
[11] H. Liu, B. Ojha, C. Morris, M. Jiang, E.P. Wojcikiewicz, P.P.N. Rao, D. Du, Positively charged chitosan and N-trimethyl chitosan inhibit Aβ40 fibrillogenesis, Biomacromolecules 16 (8) (2015) 2363−2373, https://doi.org/10.1021/acs.biomac.5b00603.
[12] J.N. Nygaard, S.P. Strand, K.M. Varum, K.I. Draget, C.T. Nordgard, Chitosan: gels and interfacial properties, Polymers 7 (3) (2015) 552–579, https://doi.org/10.3390/polym7030552.
[13] L. Rami, S. Malaise, S. Delmond, J.C. Fricain, R. Siadous, S. Schlaubitz, E. Laurichesse, J. Amedee, A. Montembault, L. David, L. Bordenave, Physicochemical modulation of chitosan-based hydrogels induces different biological responses: interest for tissue engineering, J. Biomed. Mater. Res. 102 (10) (2014) 3666−3676, https://doi.org/10.1002/jbm.a.35035.
[14] R.S.C.M.de.Q. Antonino, B.R.P.L. Fook, V.A.de.O. Lima, R.I.de.F. Rached, E.P.N. Lima, R.J. da.S. Lima, C.A.P. Covas, M.V.L. Fook, Preparation and characterization of chitosan obtained from shells of shrimp (*Litopenaeus vannamei* Boone), Mar. Drugs 15 (5) (2017) 141, https://doi.org/10.3390/md15050141.
[15] A. Montembault, C. Viton, A. Domard, Rheometric study of the gelation of chitosan in aqueous solution without cross-linking agent, Biomacromolecules 6 (2) (2004) 653−662, https://doi.org/10.1021/bm049593m.
[16] J.T. DeJong, B.M. Mortensen, B.C. Martinez, D.C. Nelson, Bio-mediated soil improvement, Ecol. Eng. 36 (2) (2010) 197–210, https://doi.org/10.1016/j.ecoleng.2008.12.029.
[17] Md.N.H. Khan, G.G.N.N. Amarakoon, S. Shimazaki, S. Kawasaki, Coral sand solidification test based on microbially induced carbonate precipitation using ureolytic bacteria, Mater. Trans. 56 (10) (2015) 1725−1732, https://doi.org/10.2320/matertrans.M-M2015820.
[18] V. Achal, Production of bacteria for structural concrete, in: F.P. Torgal, J.A. Labrincha, M.V. Diamanti, C.P. Yu, H.K. Lee (Eds.), Biotechnology and Bio Mimetic for Civil Engineers, Springer International Publishing, Switzerland 2015, p. 309−323.
[19] M. Fujita, K. Nakashima, V. Achal, S. Kawasaki, Whole-cell evaluation of urease activity of *Pararhodobacter* sp. isolated from peripheral beach rock, Biochem. Eng. J. 124 (2017) 1−5, https://doi.org/10.1016/j.bej.2017.04.004.
[20] B.M. Mortensen, M.J. Haber, J.T. DeJong, L.F. Caslake, D.C. Nelson, Effects of environmental factors on microbial induced calcium carbonate precipitation, J. Appl. Microbiol. 111 (2) (2011) 338−349, https://doi.org/10.1111/j.1365-2672.2011.05065.x.
[21] M.J. Maroney, S. Ciurli, Nonredox nickel enzymes, Chem. Rev. 114 (8) (2014) 4206−4228, https://doi.org/10.1021/cr4004488.
[22] V.S. Wfiffin, Microbial $CaCO_3$ Precipitation for the Production of Biocement, Ph.D. Dissertation Murdoch University, Western Australia, 2004.
[23] G.G.N.N. Amarakoon, S. Kawasaki, Factors affecting sand solidification using MICP with *Pararhodobacter* sp, Mater. Trans. 59 (1) (2017) 72−81, https://doi.org/10.2320/matertrans.M-M2017849.
[24] V.S. Whiffin, L.A. Van Paassen, M.P. Harkes, Microbial carbonate precipitation as a soil improvement technique, Geomicrobiol J. 24 (5) (2007) 417−423, https://doi.org/10.1080/01490450701436505.
[25] X. Wang, J. Tao, Polymer-modified microbially induced carbonate precipitation for oneshot targeted and localized soil improvement, Acta Geotech. (2018) 1–15, https://doi.org/10.1007/s11440-018-0757-z.
[26] T.H.K. Nawarathna, K. Nakashima, M. Fujita, M. Takatsu, S. Kawasaki, Effects of cationic polypeptide on $CaCO_3$ crystallization and sand solidification by microbial-induced carbonate precipitation, ACS Sustain. Chem. Eng. 6 (8) (2018) 10315–10322, https://doi.org/10.1021/acssuschemeng.8b01658.

[27] N. Hamdan, Z. Zhao, M. Mujica, E. Kavazanjian, X. He, Hydrogel-assisted enzyme-induced carbonate mineral precipitation, J. Mater. Civ. Eng. 28 (10) (2016)https://doi.org/10.1061/(ASCE)MT.1943-5533.0001604 04016089-1-9.
[28] Z. Zhao, N. Hamdan, L. Shen, H. Nan, A. Almajed, E. Kavazanjian, X. He, Biomimetic hydrogel composites for soil stabilization and contaminant mitigation, Environ. Sci. Technol. 50 (22) (2016) 12401–12410.
[29] B.N. Dzakula, L. Brecevic, G. Falini, D. Kralj, Calcite crystal growth kinetics in the presence of charged synthetic polypeptide, Cryst. Growth Des. 9 (5) (2009) 2425−2434, https://doi.org/10.1021/cg801338b.
[30] A.J. Xie, Y.H. Shen, C.Y. Zhang, Z.W. Yuan, X.M. Zhu, Y.M. Yang, Crystal growth of calcium carbonate with various morphologies in different amino acid systems, J. Cryst. Growth 285 (3) (2005) 436−443, https://doi.org/10.1016/j.jcrysgro.2005.08.039.
[31] T. Kato, Polymer/calcium carbonate layered thin-film composites, Adv. Mater. 12 (20) (2000) 1543−1546, https://doi.org/10.1002/1521-4095(200010)12:20<1543::AID-ADMA1543>3.0.CO;2-P.
[32] T. Danjo, S. Kawasaki, Microbially induced sand cementation method using *Pararhodobacter* sp. strain SO1, inspired by beach rock formation mechanism, Mater. Trans. 57 (2016) 428–437, https://doi.org/10.2320/matertrans.M-M2015842.
[33] T. Danjo, S. Kawasaki, A study of the formation mechanism of beach rock in Okinawa, Japan: toward making artificial rock, Int. J. GEOMATE 5 (1) (2013) 634–639.
[34] A.A. Qabany, K. Soga, C. Santamarina, Factors affecting efficiency of microbially induced calcite precipitation, J. Geotech. Geoenviron. 138 (8) (2012) 992−1001, https://doi.org/10.1061/(ASCE)GT.1943-5606.0000666.
[35] F.G. Ferris, V. Phoenix, Y. Fujita, R.W. Smith, Kinetics of calcite precipitation induced by ureolytic bacteria at 10 to 20°C in artificial groundwater, Geochim. Cosmochim. Acta 67 (8) (2004) 1701–1710, https://doi.org/10.1016/S0016-7037(03)00503-9.
[36] S. Dupraz, B. Menez, P. Gouze, R. Leprovost, P. Benrezeth, O.S. Pokrovsky, F. Guyot, Experimental approach of CO_2 biomineralization in deep saline aquifers, Chem. Geol. 265 (1–2) (2009) 54–62, https://doi.org/10.1016/j.chemgeo.2008.12.012.
[37] J. Mao, S. Kondu, H.F. Ji, M.J. McShane, Study of the near-neutral pH-sensitivity of chitosan/gelatin hydrogels by turbidimetry and microcantilever deflection, Biotechnol. Bioeng. 95 (3) (2005) 333−341, https://doi.org/10.1002/bit.20755.
[38] J. Kumirska, M.X. Weinhold, J. Thoming, P. Stepnowski, Biomedical activity of chitin/chitosan based materials-influence of physicochemical properties apart from molecular weight and degree of N-acetylation, Polymers 3 (4) (2011) 1875−1901, https://doi.org/10.3390/polym3041875.
[39] I. Polowczyk, A. Bastrzyk, M. Fiedot, Protein-mediated precipitation of calcium carbonate, Materials 9 (11) (2016) 1−16, https://doi.org/10.3390/ma9110944 944.
[40] J. Nie, Z. Wang, Q. Hu, Chitosan hydrogel structure modulated by metal ions, Sci. Rep. 6 (2016)https://doi.org/10.1038/srep36005.
[41] M. Benavente, Adsorption of Metallic Ions onto Chitosan: Equilibrium and Kinetic Studies, Licentiate Thesis Royal Institute of Technology Department of Chemical Engineering and Technology Division of Transport Phenomena, Stockholm, Sweden, May 2008.
[42] R.G. Pearson, Hard and soft acids and bases, HSAB, part II underlying theories, J. Chem. Educ. 45 (9) (1968) 581−587.
[43] H.F. Greer, W. Zhou, L. Guo, Reversed crystal growth of calcite in naturally occurring travertine crust, Crystals 7 (2) (2017) 36, https://doi.org/10.3390/cryst7020036.
[44] J. Wang, F. Zhang, J. Zhang, R.C. Ewing, U. Becker, Z. Cai, Carbonate orientational order and superlattice structure in vaterite, J. Cryst. Growth 407 (2014) 78–86, https://doi.org/10.1016/j.jcrysgro.2014.08.028.
[45] R.M. Wagterveld, M. Yua, H. Miedema, G.J. Witkamp, Polymorphic change from vaterite to aragonite under influence of sulfate: the “morning star” habit, J. Cryst. Growth 387 (2014) 29–35, https://doi.org/10.1016/j.jcrysgro.2013.10.044.
[46] G. Xu, Y. Tang, J. Lian, Y. Yan, D. Fu, Mineralization process of biocemented sand and impact of bacteria and calcium ions concentrations on crystal morphology, Adv. Mater. Sci. Eng. 2017 (2017) 1–13, https://doi.org/10.1155/2017/5301385 Article ID 5301385.
[47] L. Cheng, M.A. Shahin, D. Mujah, Influence of key environmental conditions on microbially induced cementation for soil stabilization, J. Geotech. Geoenviron. 143 (1) (2017) 04016083–04016091, https://doi.org/10.1061/(ASCE)GT.1943-5606.0001586.
[48] C.M. Hsu, Y.H. Huang, V.R. Nimje, W.C. Lee, H.J. Chen, Y.H. Kuo, C.H. Huang, C.C. Chen, C.Y. Chen, Comparative study on the sand bioconsolidation through calcium carbonate precipitation by *sporosarcina pasteurii* and *bacillus subtilis*, Crystals 8 (5) (2018) 189–204, https://doi.org/10.3390/cryst8050189.
[49] J. Wu, R.J. Zeng, Biomimetic regulation of microbially induced calcium carbonate precipitation involving immobilization of *sporasarcina pasteurii* by sodium alginate, Cryst. Growth Des. 17 (4) (2017) 1854–1862https://doi/abs/10.1021/acs.cgd.6b01813.
[50] C.J. Lopez, E. Caballero, F.J. Huertas, C.S. Romanek, Chemical, mineralogical and isotope behavior, and phase transformation during the precipitation of calcium carbonate minerals from intermediate ionic solution at 25°C, Geochim. Cosmochim. Acta 65 (19) (2001) 3219–3231, https://doi.org/10.1016/S0016-7037(01)00672-X.
[51] D.B. Trushina, T.V. Bukreeva, M.V. Kovalchuk, M.N. Antipina, $CaCO_3$ vaterite microparticles for biomedical and personal care applications, Mater. Sci. Eng. C 45 (2014) 644–658, https://doi.org/10.1016/j.msec.2014.04.050.
[52] Y.I. Svenskaya, H. Fattah, O.A. Inozemtseva, A.G. Ivanova, S.N. Shtykov, D.A. Gorin, B.V. Parakhonskiy, Key parameters for size- and shape-controlled synthesis of vaterite particles, Cryst. Growth Des. 18 (1) (2018) 331−337https://doi/abs/10.1021/acs.cgd.7b01328.
[53] S. Ouhenia, D. Chateigner, M.A. Belkhir, E. Guilmeau, C. Krauss, Synthesis of calcium carbonate polymorphs in the presence of polyacrylic acid, J. Cryst. Growth 310 (11) (2008) 2832–2841, https://doi.org/10.1016/j.jcrysgro.2008.02.006.
[54] G. Falini, S. Fermani, M. Gazzano, A. Ripamonti, Oriented crystallization of vaterite in collagenous matrices, Chem. Eur. J. 4 (6) (1998) 1048–1052, https://doi.org/10.1002/(SICI)1521-3765(19980615)4:6<1048::AIDCHEM1048>3.0.CO;2-U.
[55] C.R. Navarro, C.J. Lopez, A.R. Navarro, M.T.G. Munoz, M.R. Gallego, Bacterially mediated mineralization of vaterite, Geochim. Cosmochim. Acta 71 (5) (2007) 1197–1213, https://doi.org/10.1016/j.gca.2006.11.031.
[56] V. Achal, X. Pan, Influence of calcium sources on microbially induced calcium carbonate precipitation by *bacillus* sp. CR2, Appl. Biochem. Biotechnol. 173 (1) (2014) 307–317, https://doi.org/10.1007/s12010-014-0842-1.
[57] C.M. Gorospe, S.H. Han, S.G. Kim, J.Y. Park, C.H. Kang, J.H. Jeong, J.S. So, Effects of different calcium salts on calcium carbonate crystal formation by *sporosarcina pasteurii* KCTC 3558, Biotechnol. Bioprocess Eng. 18 (5) (2013) 903–908, https://doi.org/10.1007/s12257-013-0030-0.
[58] S. Liu, L. Li, Unique gelation of chitosan in an alkali/urea aqueous solution, Polymer 141 (2018) 124−131, https://doi.org/10.1016/j.polymer.2018.03.012.
[59] D. Kralj, L. Brecevic, J. Kontrec, Vaterite growth and dissolution in aqueous solution III. Kinetics of transformation, J. Cryst. Growth 177 (1997) 248−257.
[60] C. Kosanovic, G. Falini, D. Kralj, Mineralization of calcium carbonates in gelling media, Cryst. Growth Des. 11 (1) (2011) 269–277, https://doi.org/10.1021/cg1012796.
[61] B.V. Parakhonskiy, A.M. Yashchenok, S. Donatan, D.V. Volodkin, F. Tessarolo, R. Antolini, H. Mçhwald, A.G. Skirtach, Macromolecule loading into spherical, elliptical, star-like and cubic calcium carbonate carriers, ChemPhysChem 15 (13) (2014) 2817–2822, https://doi.org/10.1002/cphc.201402136.
[62] B.N. Dzakula, G. Falini, D. Kralj, Crystal growth mechanism of vaterite in the systems containing charged synthetic poly (amino acids), Croat. Chem. Acta 90 (4) (2017) 689–698, https://doi.org/10.5562/cca3290.
[63] R.N. Shafii, W. Clough, The Influence of Cementation on the Static and Dynamic Behavior of Sands, Stanford University, California, 1982.
[64] Q. Zhao, L. Li, C. Li, M. Li, F. Amini, H. Zhang, Factors affecting improvement of engineering properties of MICP-treated soil catalyzed by bacteria and urease, J. Mater. Civ. Eng. 26 (12) (2014), 04014094. https://doi.org/10.1061/(ASCE)MT.1943-5533.0001013.
[65] M.P. Harkes, L.A.V. Paassen, J.L. Booster, V.S. Whiffin, M.C.M.V. Loosdrechta, Fixation and distribution of bacterial activity in sand to induce carbonate precipitation for ground reinforcement, Ecol. Eng. 36 (2) (2010) 112−117, https://doi.org/10.1016/j.ecoleng.2009.01.004.
[66] L.A. Van Paassen, R. Ghose, T.V. Linden, W. Van der Star, M.V. Loosdrecht, Quantifying biomediated ground improvement by ureolysis: largescale biogrout experiment, J. Geotech. Geoenviron. Eng. 136 (12) (2010) 1721−1728, https://doi.org/10.1061/(ASCE)GT.1943-5606.0000382.